Synthesis and characterization of pulsed laser deposited ZnO nanorods

R .VINODKUMAR[a,b*], I. NAVAS[b], N. V. UNNIKRISHNAN[a], V. P. MAHADEVAN PILLAI[b]
[a]*School of Pure and Applied Physics, Mahatma Gandhi University, Priyadarshini Hills P.O, Kottayam-686560. Kerala*
[b]*Department of Optoelectronics, University of Kerala, Kariavattom, Thiruvananthapuram, Kerala, India – 695581*

Densily distributed ZnO nanorods have been grown by pulsed laser deposition by controlling the oxygen content during the nucleation and growth process. The XRD result suggests that ZnO nanorods are growing along the *c* axis and they are perpendicular to the surface of the substrate. Raman spectra of the as deposited ZnO nanorods support the XRD findings that the nanorod is of hexagonal wurtzite structure. AFM studies show that ZnO nanorods are densly distributed over the fused silica substrate. The transmittance of the nanorods are very high and the room-temperature photoluminescence measurements of these ZnO nanorods shown UV and visible emission. Electrical resistivity is very less compared to that of the bulk ZnO. The unique properties of ZnO nanorods may have a great potential in the application to the field-emission devices and nano-optics.

(Received January 23, 2012; accepted April 11, 2012)

Keywords: Zinc oxide nanorods, Pulsed laser deposition, Micro-Raman spectra, Temperature dependent electrical resistivity studies

1. Introduction

Zinc oxide (ZnO) is an n-type II-VI semiconductor with unique properties like wide band gap (~ 3.37 eV) and large exciton binding energy (60 meV). It is a promising material for short wavelength light emitting devices and useful for transparent electrodes in flat-panel displays and solar cells [1-3]. In recent years, semiconducting nanostructures with reduced dimensionality such as nanowires, nanorods, nanotubes etc. have importance in the optoelectronic device applications. The most recent research has been dedicated to low dimensional semiconducting nanostructures. ZnO is one of the most prominent transparent conducting oxides for advanced applications such as window layer in heterojunction solar cells, heat mirrors, piezoelectric devices, multilayer photo-thermal conversion systems and solid state gas sensors etc [4,5]. The direct optical energy gap of 3.37 eV for ZnO is large enough to transmit most of the useful solar radiation. Recent studies on ZnO has displayed a series of nanostructures with different morphologies, such as nano-needles [6], nano-belts [7,8], nano-flowers [9,10], nano-rods [10,11], nano-bows [12], nano-nails [13], nano-particles [14], nano-wires [15] and nano-wiskers [16].

ZnO nanostructures have attracted a lot of research interests due to their unique structure and size-dependent electrical, optical and mechanical properties and great potentials in a wide range of applications. This paper focuses on the fabrication of ZnO nanorods, which is useful for the assembly of nano devices and applications in light emitting and field emission devices. ZnO nanorods have been fabricated by using several deposition techniques which include chemical vapor deposition, magnetron sputtering, oxidation of an evaporated metallic film, spray pyrolysis, pulsed laser deposition (PLD), etc[17-20]. In this investigation, we report the fabrication of ZnO nanorods by pulsed laser deposition technique and their structural, optical and electrical characterization.

2. Experimental details

ZnO pellets (diameter 11mm and thickness 3 mm) are prepared from ZnO (99.99% purity, Aldrich) powder and the well sintered pellets (sintered at 1000^0C for 5 hrs) are used as targets for laser ablation. The deposition of the ZnO rods are carried out inside a vacuum chamber using a Q-switched Nd:YAG laser (Quanta-Ray INDI-series, Spectra Physics) with 532 nm radiation at a pulse width of 7 ns, repetition rate of 10 Hz and a maximum output energy of 200 mJ. ZnO thin films are fabricated using ZnO target under an oxygen ambience of 0.05 mbar on fused silica substrate kept at a substrate temperature of 873 K using laser energy of 160 mJ with duration of deposition of 30 minutes. The crystalline structure of the films are investigated by grazing incidence X-ray diffraction (GIXRD) (Siemens D5000 diffractometer) measurements using Cu *Kα* radiation at 1.5406Å wavelength. Micro-Raman spectra are recorded using Labram-HR 800 spectrometer using an excitation radiation at wavelength of 488 nm from an argon ion laser. The surface morphology of the films is investigated by AFM (Digital Instruments Nanoscope III) measurements in contact mode. Optical absorption spectra are recorded using a UV-visible double beam spectrophotometer (JASCO V-550) in the spectral range of 200 – 900 nm. Photoluminescence spectra of the samples are recorded by Horiba Jobin Yvon Flourolog III modular spectroflourometer and the resistivity measurement from 170K to 300K is done by four probe technique.

3. Results and discussion

3.1. XRD analysis

Fig. 1 shows the XRD spectrum of the ZnO nanorods prepared at an oxygen ambience of 0.05 mbar. It shows a textured crystalline nature with preferred orientation of crystal growth along [002] direction having hexagonal wurtzite structure [JCPDS card no.005-0664]. The XRD patterns suggest that the films are of superior crystalline quality. As the substrate temperature increases the adatom mobility and hence kinetic energy of the species increases and they get diffused through the lattice and get deposited at appropriate lattice location to get stoichiometric, good quality films. This result suggests that ZnO nanorods are growing along the *c* axis and they are perpendicular to the surface of the substrate.

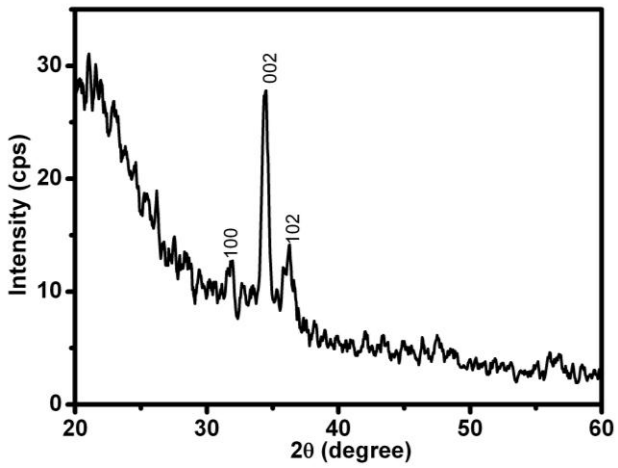

Fig. 1. XRD spectra of laser ablated ZnO nanorods.

3.2. AFM analysis

Fig. 2 represents two dimensional AFM images of the ZnO nanorods on a scan area of 5 µm x 5 µm and 2µm x 2µm. The data are measured in 256x256 pixel format and the scan rate is at 5.086 Hz. For the grain size calculation 4-5 frames are selected and 20 measurements are taken in each frame with an accuracy of ± 4 nm. The AFM image of the film prepared at substrate temperatures 873K shows a densely packed distribution of nanorods with well–defined grain boundary. At high temperature, the nucleation of ZnO islands on the surface of substrates depends strongly on the amount of active oxygen. When grown in 90% oxygen plasma, ZnO has a high nucleation density and forms sufficient active oxygen species are provided around the substrates so that the ZnO nanorod formation is enhanced. The rms surface roughnesses of the nonorods are 71.25 nm.

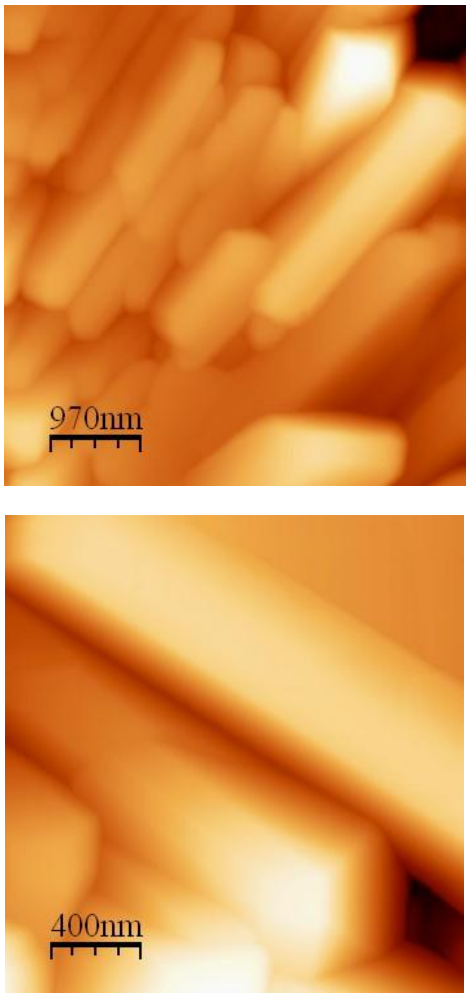

Fig. 2. AFM image of laser ablated ZnO nano rods.

3.3. Micro-Raman studies

Fig. 3 shows the Raman spectra of the ZnO nanoroads. ZnO has a hexagonal wurtzite structure and belongs to the space group $P6_3mc$ (C_{6v}^4) with two formula units in the primitive cell. All the atoms occupy the C_{3v} sites. The group theoretical calculation based on the correlation method suggested by Fateley et al., [21] predicts nine optical modes which are distributed as follows:

$$\Gamma_{ZnO}^{optrical} = A_1(IR,R) + 2B_2 + E_1(IR,R) + 2E_2(R)$$

where A_1 and E_1 modes are active in both Raman and IR spectra whereas E_2 modes are active only in Raman spectrum and B_2 mode is inactive in both Raman and IR spectra. Based on earlier Raman investigations the different Raman modes of the ZnO films can be expected as follows: A_1-TO modes ~ 382 cm^{-1}, E_1 -TO modes ~

407 cm^{-1}, A_1 - LO modes ~ 576 cm^{-1}, E_1 -LO modes ~ 587 cm^{-1}, E_2 - low modes ~ 102 $cm^{-1}$and E_2 - high modes ~ 438 cm^{-1} [22]. The low frequency E_2 mode is associated with the vibration of the heavy Zn sub- lattice, while the high frequency E_2 mode involves only the oxygen atoms [22].

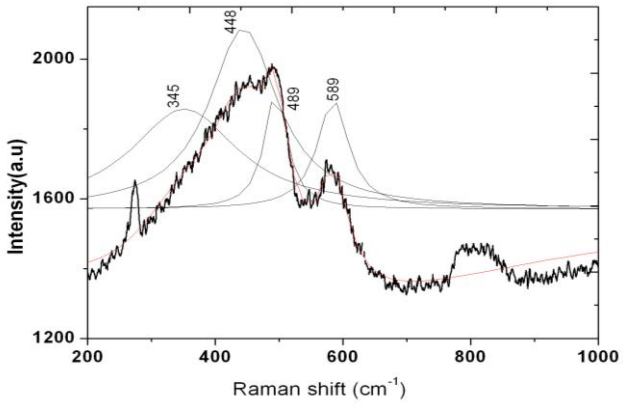

Fig. 3. Micro Raman spectra of the ZnO nano road.

In the Raman spectrum of the ZnO nanorods prepared at a substrate temperature 873 K, A_1 -LO mode appears with a medium intensity at 589 cm^{-1}. The broad spectral feature extending from 350 to 500 cm^{-1} on deconvolution yield three bands at 345, 448 and 489 cm^{-1}. The 448 cm^{-1} band can be due to E_2 - high mode. The shifting of A1 (LO) mode to higher wave number value and the broad spectral feature suggests the presence of distorted tetrahedra in the film. The band ~489 cm^{-1} is due to the contribution from Si-Si stretching vibrations of the fused silica substrate.

3.4. Optical properties

Fig. 4 shows the transmittance spectra of ZnO nanorods in the wavelength range of 200–900 nm. The average transmittance for the films in the wavelength range 400-900 nm is 89%. The sharp fall of transmittance at the absorption edge (~370 nm) of the films shows the crystalline and direct band gap nature of the film. The optical band gap E_g can be estimated from the Tauc plot:

$$(\alpha h\nu) = \mathrm{A}(h\nu - E_g)^n$$

where E_g is the band gap corresponding to a particular transition occurring in the film, A is a band edge constant, ν is the transition frequency and the exponent n characterizes the nature of band transition. n =1/2 and 3/2 corresponds to direct allowed and direct forbidden transitions respectively and n =2 and 3 corresponds to indirect allowed and indirect forbidden transitions, respectively [23-27]. The optical band gap E_g can then be obtained from the intercept of $(\alpha h\nu)^2$ vs $h\nu$ for direct transitions. It is observed that for the ZnO nanorods, the best straight line is obtained for n = 1/2, which is expected for direct allowed transition. The calculated value of the band gap energy is 3.22 eV which is less than that of the bulk ZnO.

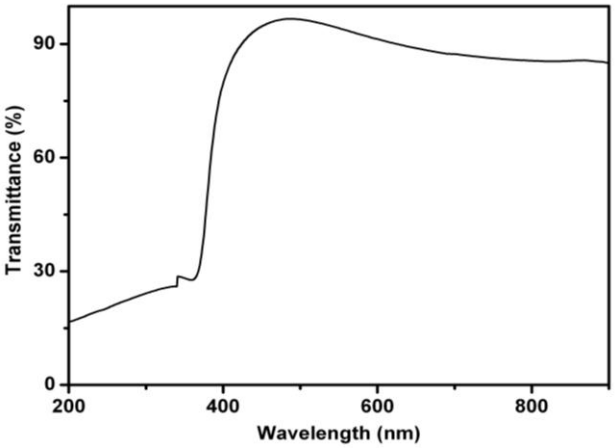

Fig. 4. Transmittance spectra of laser ablated ZnO nanorods.

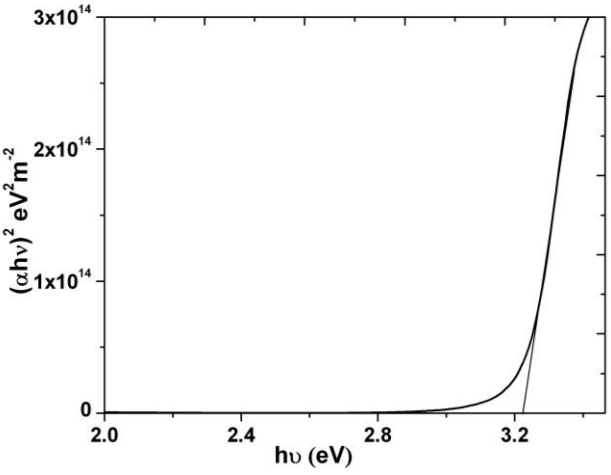

Fig. 5. Tauc plot of the laser ablated ZnO nanorods.

3.5. Photoluminescence studies

Fig. 6 shows the room temperature PL spectra of the ZnO nanorods excited at a wavelength of 325 nm. The PL emission from ZnO is classified in to two types. One is the UV emission of the near band edge related to free-exciton recombination and the other is the deep-level (DL) emission in the visible range. The deep level emission in the visible region is attributed to structural defects such as oxygen vacancies and interstitial zinc [28, 29].

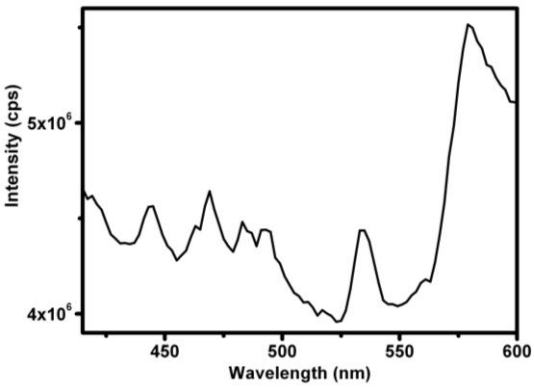

Fig. 6. PL spectra of pulsed laser deposited ZnO nanorods.

PL measurements show only visible emission for ZnO nanorods grown on quartz substrates on oxygen ambience. The intensity of the visible PL peak increases significantly while the UV emission is suppressed due to large competition from the defect emission. Preparation of nanorods at higher substrate temperature reveals that oxygen interstitials are responsible for the orange-red emission. In pure oxygen ambience at high temperature, new defects of oxygen interstitials are created. Lattice matching between ZnO and substrates, electric field enhancement and the amount of defects in the starting nuclei are found to be important to the self-alignment of nanorods [30]. This can be of great research interests in constructing two-dimensional photonic crystals.

3.6. Electrical properties

The undoped ZnO films generally do not show any appreciable electrical conductivity. The high dc electrical resistance, in the order of MΩ, is reported for ZnO films at 300 K by sahay et al., and they have attributed this high resistance to the large density of extrinsic traps at the grain boundaries due to oxygen chemisorptions [31]. The traps can deplete the grains and result in a charge carrier barrier at the grain boundaries [32]. The dc resistance of the ZnO nanorods in the temperature range 170–300 K is measured using four-probe method. The ZnO nanorods show an electrical resistivity equal to 1.84×10^{-1} Ωm at 300K which is less compared to that of ZnO thin films [31].

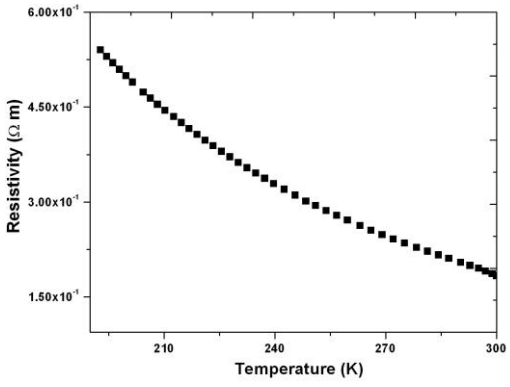

Fig. 7. DC resistivity variation over temperature of pulsed laser ablated ZnO nanorods.

4. Conclusion

The structural, optical and electrical properties of ZnO nanorods grown on fused silica substrates by PLD were investigated. The observation of the high-frequency E_2 mode and the longitudinal optical A_1 (LO) mode in the Raman spectra supports the XRD findings that the nanorod is of hexagonal wurtzite structure. AFM images show densly disytributed ZnO nanorods. The films are showing good transparency in the visible region and the band gap energy is less compared to that of bulk ZnO. The PL spectra show an enhanced visible emission. The dc electric resistivity of the ZnO nanoroads is less than that of the ordinary films. It is concluded that the microstructure, electrical and emission properties of the ZnO nanorods grown on fused silica substrates by PLD are of great importance in the optical and optoelectronic device applications.

Acknowledgement

One of the authors N. V. Unnikrishnan is thankful to UGC, Govt. of India for financial assistance through SAP-DRS program, R. Vinodkumar wishes to express his immense gratitude to the University Grants Commission (UGC), India for providing Dr. D.S. Kothari Post Doctoral Fellowship.

Refernces

[1] K. Elmer J. Phys. D: Appl. Phys,. 33, R 17(2000).
[2] M. Krunks, E. Mellikov, Thin Solid Films. **270**, 33 (1995).
[3] J. A. Aranovich, D. Golmaya, A. L. Fahrenbruch, R. H. Bube. J. Appl. Phys. **51**, 4260 (1980).
[4] P. P. Sahay, J. Mat. Sci. **40**, 4383 (2005).
[5] P. P. Sahay, S. Tewari, S. Jha, M. Shamsuddin, J. Mat. Sci. **40**, 4791 (2005).
[6] W. I. Park, G. C. Yi, M. Y. Kim, S. J. Pennycook, Adv. Mater. **15**, 526 (2003).
[7] M. H. Huang, S. Mao, H. Feick, H. Yan, Y. Wu, H. Kind, E. Weber, R. Russo, P. Yang, Science **292**, 1897 (2001).
[8] Z. W. Pang, Z. R. Dai, Z. L. Wang, Science **291**, 1947 (2001).
[9] J. Zhang, L. D. Sun, X. C. Jiang, C. S. Liao, C. H. Yan, Cryst. Growth Des. **4**, 309 (2004).
[10] J. Du, Z. Liu, Y. Huang, Y. Gao, B. Han, W. Li, G. Yang, J. Cryst. Growth **280**, 126 (2005).
[11] B. P. Zhang, N. T. Binh, K. Wakatsuki, Y. Segawa, Y. Kashiwaba, K. Haga, Nanotechnology **15**, S382 (2004).
[12] W. Hughes, Z. L. Wang, J. Am. Chem. Soc. **126**, 6703 (2004).
[13] J. Y. Lao, J. Y. Huang, D. Z. Wang, Z. F. Ren, Nano Lett. **3**, 235 (2003).
[14] Y. Yang, H. Chen, B. Zhao, X. Bao, J. Cryst. Growth **263**, 447 (2004).
[15] H. Q. Yan, R. R. He, J. Johnson, M. Law, R. J. Saykally, P. D. Yang, J. Am. Chem. Soc. **125**, 4728

(2003).
[16] J. Wang, L. Gao, J. Cryst. Growth **262**, 290 (2004).
[17] J. H. Lee, B. O. Park, Thin Solid Films **426**, 94 (2003).
[18] M. Jung, J. Lee, S. Park, H. J. Chang, J. Cryst. Growth **283**, 384 (2005).
[19] Haga, T. Suzuki, Y. Kashiwaba, H. Watanabe, H. P. Zhang, Y. Segawa, Thin Solid Films **433**, 131 (2005).
[20] J. L. Zhao, X. M. Li, J. M. Bian, W. D. Yu, X. D. Gao, J. Cryst. Growth **276**, 507 (2005).
[21] William G. Fateley, Francis R. Dollish, Neil T. Mc Devitt, Freeman F. Bentley, Infrared and Raman Selection Rules for Molecular and Lattice Vibrations – The Correlation Method.. Wiley-Interscience, New York 1972.
[22] U. Ozgür, Ya. I. Alivov, C. Liu, A. Teke, M. A. Reshchikov, S. Dogan, V. Avrutin, S. J. Cho, H. Morkoc, J. Appl. Phys. **98**, 041301 (2005).
[23] A. Goswami, Thin Film Fundamentals, New Age International (p) Limited, New Delhi, 1996.
[24] J. Pankove, Optical Process in Semiconductors, Dover Publication, New York, 1971.
[25] J. R. Rani, V. P. Mahadevan Pillai, R. S. Ajimsha, M. K. Jayaraj, R. S. Jayasree, J. Appl. Phys. **100**, 014302 (2006).
[26] K. J. Lethy, D. Beena, R. Vinodkumar, V. P. Mahadevan Pillai, Applied Surface Science, **254**, 2369 (2008).
[27] M. Suchea, S. Christoulakis, M. Katharakis, G. Kiriakidis, N. Katsarakis, E. Koudoumas, Applied Surface Science, **253**, 8141 (2007).
[28] S. Dutta, S. Chattopadhyay, M. Sutradhar, A. Sarkar, M. Chakrabarti, D. Sanyal, D. Jana, J. Phys. Condens. Matter, **19**, 236218 (2007).
[29] Z. K. Tang, G. K. L. Wong, P. Yu, Appl. Phys. Lett. **72**, 3270 (1998).
[30] Xiang Liu, Xiaohua Wu, Hui Cao, R. P. H. Chang, J. Appl. Phys., **95**, 3141 (2004).
[31] P. P. Sahay, S. Tewari, R. K. Nath, Cryst. Res. Technol. **42**, 723 (2007).
[32] H. Demiryont, K. E. Nietering, Sol.Energ. Mat. **19**, 79 (1989).

*Corresponding author: vinodkopto@gmail.com